European Journal of Pharmaceutics and Biopharmaceutics 88 (2014) 635–642

Contents lists available at ScienceDirect

European Journal of Pharmaceutics and Biopharmaceutics

journal homepage: www.elsevier.com/locate/ejpb

Research paper

In vitro assessment of biopolymer-modified porous silicon microparticles for wound healing applications

Michela Mori [a,1], Patrick V. Almeida [b,1], Michela Cola [a,b,1], Giulia Anselmi [a,b], Ermei Mäkilä [b,c], Alexandra Correia [b], Jarno Salonen [c], Jouni Hirvonen [b], Carla Caramella [a,*], Hélder A. Santos [b,*]

[a] Department of Drug Sciences, University of Pavia, Italy
[b] Division of Pharmaceutical Chemistry and Technology, Faculty of Pharmacy, University of Helsinki, Finland
[c] Laboratory of Industrial Physics, Department of Physics and Astronomy, University of Turku, Finland

ARTICLE INFO

Article history:
Received 19 July 2014
Accepted in revised form 29 September 2014
Available online 8 October 2014

Keywords:
In vitro
Microparticles
Porous silicon
Biopolymers
Drug delivery
Chitosan
Hyaluronic acid

ABSTRACT

The wound healing stands as very complex and dynamic process, aiming the re-establishment of the damaged tissue's integrity and functionality. Thus, there is an emerging need for developing biopolymer-based composites capable of actively promoting cellular proliferation and reconstituting the extracellular matrix. The aims of the present work were to prepare and characterize biopolymer-functionalized porous silicon (PSi) microparticles, resulting in the development of drug delivery microsystems for future applications in wound healing. Thermally hydrocarbonized PSi (THCPSi) microparticles were coated with both chitosan and a mixture of chondroitin sulfate/hyaluronic acid, and subsequently loaded with two antibacterial model drugs, vancomycin and resveratrol. The biopolymer coating, drug loading degree and drug release behavior of the modified PSi microparticles were evaluated *in vitro*. The results showed that both the biopolymer coating and drug loading of the THCPSi microparticles were successfully achieved. In addition, a sustained release was observed for both the drugs tested. The viability and proliferation profiles of a fibroblast cell line exposed to the modified THCPSi microparticles and the subsequent reactive oxygen species (ROS) production were also evaluated. The cytotoxicity and proliferation results demonstrated less toxicity for the biopolymer-coated THCPSi microparticles at different concentrations and time points comparatively to the uncoated counterparts. The ROS production by the fibroblasts exposed to both uncoated and biopolymer-coated PSi microparticles showed that the modified PSi microparticles did not induce significant ROS production at the concentrations tested. Overall, the biopolymer-based PSi microparticles developed in this study are promising platforms for wound healing applications.

1. Introduction

In the last decades, intensive research has led to study the complexity of events involved on the wound healing process, which is a regenerative tissue process mediated by different and interdependent cellular events, with the aim of promoting the cellular and extracellular matrix (ECM) proliferation, therefore re-establishing the integrity of the damaged tissue [1]. The wound healing starts immediately after the lesion through the release of a pool of molecules at the injury site, including cytokines, proteins and growth factors. These series of events, frequently referred as homeostasis, lead to the formation of a clot in the wound [2]. At this point, the wound healing process starts, which is characterized by three overlapping phases: inflammation, proliferation and scar maturation [3,4].

Some biopolymers, including chitosan (CHI), chondroitin sulfate (CS) and hyaluronic acid (HA), are well-known in the pharmaceutical field, not only for their bioadhesive, biocompatibility and non-toxic properties, but also for promoting the tissue repairing process [5–7]. Due to their unique intrinsic properties, these biopolymers have been used over the years in a wide number of

Abbreviations: ATR-FTIR, attenuated total reflectance Fourier transform infrared; CHI, chitosan; CS, chondroitin sulfate; DMEM, Dulbecco's modified Eagle's medium; ECM, extracellular matrix; FTIR, Fourier transform infrared; GAGs, glycosaminoglycans; HA, hyaluronic acid; HBSS, Hank's buffer saline solution; HPLC, high-performance liquid chromatography; MES, 2-(N-morpholino)ethanesulfonic acid; PSi, porous silicon; ROS, reactive oxygen species; RSV, resveratrol; SEM, scanning electron microscopy; THCPSi, thermally hydrocarbonized porous silicon; VCM, vancomycin.

* Corresponding authors. Department of Drug Sciences, University of Pavia, Viale Taramelli 12, 27100 Pavia, Italy. Tel.: +39 0382 987385 (C. Caramella). Division of Pharmaceutical Chemistry and Technology, Faculty of Pharmacy, FI-00014 University of Helsinki, Finland. Tel.: +358 2941 59661 (H.A. Santos).

E-mail addresses: carla.caramella@unipv.it (C. Caramella), helder.santos@helsinki.fi (H.A. Santos).

[1] These authors contributed equally to this work.

http://dx.doi.org/10.1016/j.ejpb.2014.09.010
0939-6411/

biomedical applications, including controlled delivery of pharmaceuticals (e.g., antimicrobials [8] and healing enhancers [9]).

CHI possesses unique features including adsorptive and bioadhesive properties, as well as antimicrobial and antifungal effects. This polymer is biocompatible, biodegradable, non-toxic and a renewable material [10,11]. The polycationic nature of CHI enables it to interact with the negatively charged surfaces, such as mucosal membranes and microorganism surfaces. In addition, one of the most relevant biomedical applications of CHI is its potential in drug delivery [10], which together with its intrinsic hemostatic, anti-inflammatory, antimicrobial and wound-healing effects, may be exploited in wound care and management, especially to prevent or treat wound infections (e.g., open-skin wound and burn infections) [11]. CHI alone or associated/incorporated into dressings and topical formulations [2], may be used as a carrier to deliver a wide range of biopharmaceuticals into the wound, including antimicrobials [8,12], and growth factors [9,13], thus enhancing wound healing. This permits a local administration of biopharmaceuticals, overcoming the problems of the systemic administration of antibiotics, as well as the sustained bioavailability related problems of growth factors.

Another family of native biopolymers widespread in the ECM are the glycosaminoglycans (GAGs), which represent the negatively charged polysaccharides at the cell membranes. The remarkable properties of GAG-based compounds, such as chondroitin sulfate (CS), hyaluronic acid (HA), chondroitin, dermatan, heparin/heparin, and keratin, have rendered these biomaterials promising for application in tissue engineering and wound healing, owing to their several biological functions [14]. On the one hand, GAGs can be found free in the ECM, thus interacting with other components of the ECM and, consequently, maintaining the normal structural and functional integrity of the connective tissue, carrying out a chondroprotective function. On the other hand, GAGs can be displayed on the cells' surface [5] and interact with the proteins regulating several biological processes, such as cellular activation, proliferation and differentiation as well as inflammation [15,16]. For example, CS plays an important role in wound healing [17], accelerating the healing process by regulating the fibroblasts proliferation and the rate of wound closure [14], as well as supporting granulation tissue formation [3].

Similar to CS, exogenous HA may have chondroprotective effects *in vivo* [18], as it can be incorporated into the cartilage [19], enhancing the chondrocyte, HA and proteoglycan's synthesis, as well as fibroblast proliferation. Additionally, HA can act as anti-inflammatory and anti-scavenger [4]. HA is highly biocompatible, biodegradable, non-toxic, non-antigenic and non-immunogenic [20]. It is known that HA is involved in several mechanisms of the wound healing process. For example, it has been demonstrated that it improves and accelerates the wound healing of chronic wounds [21].

Porous silicon (PSi) is an inorganic Si-based material with well-defined structure and surface chemistries [22–24]. PSi is characterized by its unique properties, such as large surface area, high pore volume, controllable pore sizes and surface chemistry [24,25]. In addition, PSi can be made thermally stable in a biological environment, mechanically resistant, and is relatively inexpensive [22,23]. Moreover, PSi is non-toxic, biocompatible, biodegradable, and allow high payloads and variable release kinetics for controlled drug delivery formulations [24–31]. Therefore, PSi materials can be considered as excellent candidates for drug delivery applications.

The aim of this work was to prepare and characterize thermally hydrocarbonized PSi (THCPSi) microparticles coated with biopolymers (CHI and CS/HA) and loaded with two antibacterial drug compounds, vancomycin (VCM) [32] and resveratrol (RSV) [33,34], in order to develop drug delivery microsystems for potential future applications in wound healing. We have also evaluated the *in vitro* toxicity and oxidative stress of the prepared composites in fibroblast cells. Synthetic materials, such as PSi microparticles, may be loaded with drug compounds [35] and subsequently biofunctionalized with CHI [10], CS [36] and HA [37], imparting them additional advantageous properties for drug delivery applications. Furthermore, these biopolymers may promote and accelerate the wound healing by enhancing the proliferation of fibroblasts, which play a key role in the wound healing process. The study herein is focused on the overall physicochemical characterization as well as the *in vitro* safety evaluation of the developed microparticulate platforms, which by encompassing various relevant biomaterials, are expected to endow promising features for wound healing applications.

2. Materials and methods

2.1. Preparation and characterization of the mesoporous silicon (PSi) microparticles

Silicon wafers Si ⟨100⟩, of p+-type with resistivity values of 0.01 – 0.02 Ω cm were used in the preparation of the PSi microparticles as described elsewhere [28,38]. Briefly, the PSi microparticles were prepared by anodizing the wafers with a constant current density of 50 mA/cm^2 in hydrofluoric acid (Merck, 40%)–ethanol (Altia Oyj 99.5%) mixture (1:1). Free-standing films were obtained by sharply increasing the current intensity. The free-standing PSi films were then ball milled in an agate grinding jar. The obtained particles were dry-sieved using a test sieve with nominal pore sizes of 25, 53 and 75 μm. The milling and sieving cycles were repeated several times to achieve the desired particle sizes of 25–53 and 53–75 μm. After the dry-sieving, the particles were rinsed with ethanol on the mesh in order to remove small agglomerates. Prior to the surface treatments, the sieved particles were immersed into a hydrofluoric acid solution to remove the oxides formed during the milling and subsequently dried at 65 °C. After drying, the microparticles were thermally hydrocarbonized under a N_2/acetylene (1:1) flow at 500 °C for 15 min using a process described in detail elsewhere to form thermally hydrocarbonized porous silicon (THCPSi) microparticles [29,39].

The physical properties of the PSi microparticles were characterized by N_2 sorption at 77 K using a TriStar 3000 gas sorption apparatus (Micromeritics Inc., USA). The specific surface area was calculated from the adsorption isotherm using the Barrett–Joyner–Halenda (BJH) [6] and Brunauer–Emmet–Teller (BET) theories [40]. The pore volume was estimated from the total adsorbed amount at a relative pressure of $p/p_0 = 0.97$ [41]. The average pore diameter was estimated using the obtained values for the specific surface area and the total pore volume, assuming the pores are cylindrical.

2.2. Biopolymer coating of the THCPSi microparticles

THCPSi microparticles were coated with CHI and a mixture of CS and HA (ratio 2:1, CS:HA) at a ratio of 3:1 (particles:biopolymers). CHI solution was prepared in 1% (v/v) acetic acid (Fluka, Biochemika) aqueous solution, at a concentration of 7.5 mg/mL. CS and HA solutions were prepared in MilliQ-water (Merck Millipore) at concentrations of 7.5 and 3.75 mg/mL, respectively. After 24 h of stirring at ~800 rpm and at room temperature, the particles were collected, centrifuged (Centrifuge 5415 D, Eppendorf) at 13,000 rpm for 3 min, washed twice with Milli-Q water, and dried at room temperature after the removal of the supernatant.

2.3. Fourier transform infrared (FTIR) analysis

The successful coating of the surface of the THCPSi microparticles with the biopolymers was studied by attenuated total

reflectance (ATR)-FTIR. The ATR-FTIR spectra of the THCPSi microparticles were obtained using a Bruker VERTEX 70 series FTIR spectrometer (Bruker Optics, Germany) with a horizontal ATR sampling accessory (MIRacle, Pike Technology, Inc.). The ATR-FTIR spectra were recorded at the wavenumber region of 4000–650 cm^{-1} with a resolution of 4 cm^{-1} at room temperature. Prior to each measurement, the microparticles were left to dry at room temperature for 24 h.

2.4. Scanning electron microscopy (SEM)

The morphology of the microparticles was investigated using a SEM (Zeiss DSM 962). The microparticles were placed on the stubs and then sputter coated with platinum prior to imaging.

2.5. Drug loading

The coated and uncoated THCPSi particles, with a particle size fractions of 25–53 and 53–75 μm, were loaded with resveratrol (RSV) and vancomycin (VCM). The drug loading of the PSi particles with RSV was performed by an immersion method, in which the bare and coated THCPSi particles were immersed in 10 mg/mL of RSV dissolved in ethanol and stirred for 1.5 h. In the case of VCM, the coated and uncoated THCPSi microparticles were loaded with the drug at a ratio of 1:2 (particles:drug), by immersion of the particles in an aqueous drug solution (10 mg/mL). After 90 min of stirring at ~400 rpm at room temperature, the particles were collected, centrifuged at 8000 rpm for 4 min, and dried at room temperature after the removal of the supernatant. The supernatant was then analyzed by high-performance liquid chromatography (HPLC) as described below.

2.6. Determination of drug loading degree by HPLC analysis

The loading degree of RSV and VCM loaded inside the coated and uncoated THCPSi microparticles was determined by first extracting the drugs loaded inside the particles, using 10 mL of ethanol under stirring for 1 h. The amount of RSV and VCM loaded into the THCPSi microparticles was determined by HPLC (Agilent 1260, Agilent Technologies) as follows. For RSV, a Gemini-NX column (Phenomenex®) 3 μm, C_{18}, 110 Å (4.60 × 100 mm), with a mobile phase consisting of phosphoric acid (Sigma–Aldrich) and acetonitrile (VWR International) at a ratio of 75:25% (V/V), an injection volume of 20 μL, a flow rate of 1.2 mL/min and a λ = 305 nm, were used. The amount of RSV loaded into the THCPSi microparticles was determined using a HPLC method with a calibration curve of $y = 138.25x + 0.75519$ and R^2 of 0.9999. For VCM, the measurements were made using a Gemini-NX column (Phenomenex®) 3 μm, C_{18}, 110 Å (4.60 × 100 mm), with a mobile phase consisting of trifluoroacetic acid (Sigma–Aldrich) and acetonitrile (VWR International) at a ratio of 85:15% (V/V), an injection volume of 50 μL, a flow rate of 1.5 mL/min and a λ = 229 nm. The amount of RSV loaded into the THCPSi microparticles was determined using a HPLC method with a calibration curve of $y = 47.875x$ and a R^2 of 0.9997.

2.7. Drug release experiments

The release profiles of RSV and VCM from the PSi particles were compared to the dissolution of pure drugs. The *in vitro* dissolution tests were conducted in medium at pH 5.5 to mimic the conditions of the skin [42]. The medium at pH 5.5 was prepared using 2-(N-morpholino)ethanesulfonic acid (MES) (Sigma–Aldrich). The release test was carried out in a volume of 100 mL, which was kept under stirring at 200 rpm and at 32 ± 1 °C. The volume withdrawn for HPLC analysis was 1 mL and for each time point, and the volume was replaced with 1 mL of the buffer solution pre-warmed at 32 ± 1 °C. Samples were collected after 5, 10, 15, 20, 30, and 60 min. The release tests of each sample were repeated for at least four times. The quantification of the drug released from the THCPSi microparticles was performed by HPLC, as described above.

2.8. Cell culturing

Fibroblast cells isolated from human neonatal foreskin (CCD-1112Sk, ATCC® CRL-2429™) were used as an *in vitro* cell model. The cells were stored in liquid nitrogen at 77 K. Fibroblast cells were fed with 10% heat inactivated fetal bovine serum (HIFBS, HyClone)-Dulbecco's Modified Eagle Medium (DMEM, HyClone) medium, 1% non-essential amino acids (HyClone), 1% L-glutamine (EuroClone SpA), penicillin (100 IU/mL, EuroClone SpA), streptomycin (100 mg/mL, EuroClone SpA), and sodium pyruvate (Life Technologies). The cell cultures were kept in a standard incubator (16 BB gas, Heraeus Instruments GmbH) at 37 °C in an atmosphere of 5% CO_2 and 95% relative humidity. Prior to each test, the cells were harvested with 0.25% (v/v) trypsin-phosphate buffer solution–ethylenediamine tetraacetic acid solution.

2.9. Cell viability/proliferation studies

The cell viability/proliferation assay was used to determine the toxicity/proliferation of the cells when exposed to the uncoated and biopolymer-coated PSi microparticles at different experimental conditions. About 2×10^4 cells/well of fibroblasts cell suspensions in culture medium were seeded in 96-well plates (Corning Inc.) and allowed to attach overnight. Then, the medium was removed and the plates were washed once with Hank's buffer saline solution (HBSS, pH 7.4). After washing, each sample solution of bare THCPSi particles and with biopolymer-coated THCPSi particles coated (CHI, and mixture of CS/HA) was added into each well, and the plates were incubated for 24, 48, 72, and 96 h. The biopolymer-coated and uncoated particles were prepared in four different concentrations (1000, 500, 100, and 25 μg/mL) using cell medium (without phenol red). DMEM and Triton® X-100 (1%, Merck KGaA) were used as positive and negative controls, respectively. At each time point, the medium was carefully removed from the wells and the plates were washed twice with HBSS (pH 7.4). Then, 50 μL of HBSS (pH 7.4) and 50 μL of CellTiter-Glo® reagent (Promega Corporation) were added to each well. After mixing with an orbital shaking for ~2 min to induce cell lysis, the plate was left for ~15 min at room temperature. Finally, the luminescence was measured with a Varioskan Flash spectral scanning multimode reader (Thermo Fisher Scientific Inc.).

2.10. Reactive oxygen species (ROS) assay

ROS production assay was used to monitor the generation of ROS that are essential intermediates in oxidative metabolism. However, when generated in excess due to a variety of cell stresses, ROS can damage cells contributing to inflammation and tissue damage. A fluorescent-based method based on 2,7-dichlorofluorescein-diacetate (DCF-DA, Sigma–Aldrich) compound was used to detect and quantify intracellular H_2O_2 production. The ROS production by the cells treated with the samples was compared to the cells treated with the H_2O_2 control (0.09%) [29]. Bare THCPSi particles (25–53 μm) and THCPSi particles coated with biopolymers (CHI, and mixture of CS/HA) solutions were prepared in three different concentrations (25, 100, and 500 μg/mL) in HBSS medium (pH 7.4). DCF-DA was dissolved in 15–20 μL of dichloromethane (DCM, Sigma–Aldrich) and HBSS (pH 7.4) was added to adjust the final volume. Before use, DCM was evaporated in a vacuum oven (Haraeus vacutherm, Kelvitron®).

About 100 μL of 2×10^5 cells/mL of fibroblasts cell suspensions in DMEM medium was seeded in 96-well plates and allowed to attach overnight. Then, the medium was removed and the plate was washed once with 100 μL of HBSS (pH 7.4). After washing, 100 μL of 10 μM DCF-DA solution was added to each well and the plate was incubated for 1 h at 37 °C. After the solution removal and plate washing, 100 μL of each sample solution was added to each well, and the plate was then incubated for 6 h at 37 °C. The DCF fluorescence was measured with a Varioskan Flash instrument (excitation λ = 498 nm and emission λ = 522 nm).

2.11. Statistical analysis

Results are expressed as the mean ± standard deviation (s.d.) of at least three independent measurements. When indicated, the experimental values were statistically analyzed by means of the Student's *t*-test with the level of significance set at probabilities of $^{*}p < 0.05$ and $^{**}p < 0.01$. The analysis was performed using GraphPad Prism 5 software (GraphPad Software Inc.).

3. Results and discussion

3.1. Characterization of the THCPSi microparticles

In order to evaluate the effect of the particle size, two different particle size fractions were prepared according to the nominal sieve mesh limits of 25–53 and 53–75 μm [27]. The THCPSi microparticles obtained presented a specific surface area of 476 m^2/g, a pore volume of 1.27 cm^3/g, and an average pore diameter of 12.9 nm.

The THCPSi microparticles were subsequently coated by adsorption of CHI [43] and a mixture of CS/HA [44] on the microparticles' surface. Additionally to the proposed mechanism of adsorption for the biopolymeric coating of the THCPSi microparticles, an electrostatic interaction between the microparticles and the positively charged CHI or the negatively charged GAG polymers (CS and HA) may occur. In order to evaluate the adsorption of the biopolymers onto the surface of the THCPSi microparticles, FTIR analysis was performed. Fig. 1 shows the ATR-FTIR spectra of the bare THCPSi microparticles, biopolymers alone and biopolymer-coated microparticles (CHI-THCPSi and CS/HA-THCPSi). The FTIR spectrum of the THCPSi microparticles (Fig. 1i and iv) showed several distinctive features, such as the Si back-bonded C–H_x groups at around 1000 cm^{-1}, and the Si–C bonds at 800 cm^{-1} [39]. The major features of the FTIR spectrum of CHI (Fig. 1iii) are the bands at 3455 cm^{-1} (–OH stretch), 2867 cm^{-1} (C–H stretch), 1589 cm^{-1} (N–H bend), 1154 cm^{-1} (bridge C–O stretch), and 1094 cm^{-1} (C–O stretch) [45]. The main characteristic bands of the FTIR spectra of CS and HA (Fig. 1vi and vii) are at 1610 and 1411 cm^{-1} ($-COO^-$), at 1240 cm^{-1} the groups SO_4^{2-}, and in the range of 1000–1200 cm^{-1} the sugar groups [46,47]. Comparing the FTIR spectra of the uncoated microparticles (Fig. 1i and iv) to the biopolymers (Figs. 1iii, vi and vii), and to the biopolymer-coated THCPSi microparticles (Figs. 1ii and v), it is noticeable that the biopolymers' FTIR spectra features are superimposed on the bare particles' spectrum. Indeed, new bands have emerged on the FTIR spectra of coated particles (corresponding to the biopolymers), particularly the band at 1153 cm^{-1} for CHI-THCPSi (Fig. 1ii), and at 1651, 1518, and 1153 cm^{-1} for CS/HA-THCPSi (Fig. 1v) microparticles. Moreover, the broad absorption bands of the uncoated THCPSi particles were also observed in the FTIR spectra corresponding to their coated counterparts, therefore confirming the adsorption of the biopolymers onto the surface of the particles and the successful biopolymer-coating of the THCPSi microparticles.

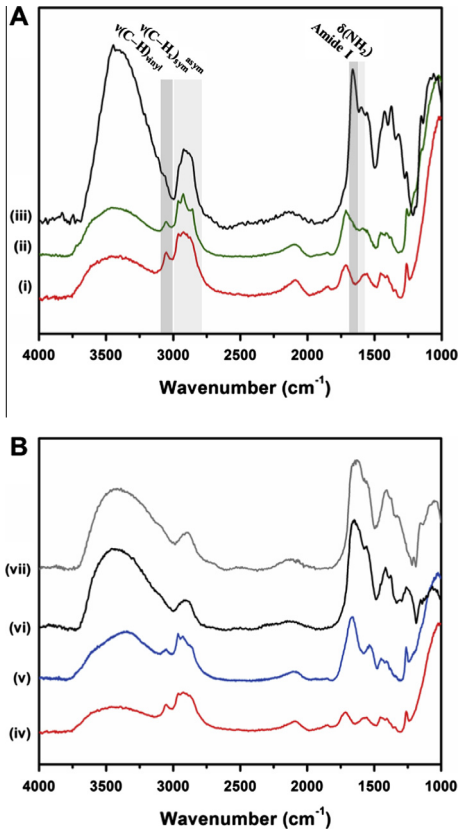

Fig. 1. ATR-FTIR spectra of THCPSi microparticles (i; iv), CHI-THCPSi microparticles (ii), CHI (iii), CS/HA-THCPSi microparticles (v), CS (vi), and HA (vii). The relevant features of each spectrum are highlighted for clarity. (For interpretation of the references to color in this figure legend, the reader is referred to the web version of this article.)

In addition, the surface of the THCPSi microparticles was also examined by SEM imaging. For example, Fig. 2 shows the SEM pictures of the bare THCPSi microparticles and the biopolymer-coated microparticles (CHI-THCPSi and CS/HA-THCPSi). Comparing the morphological appearance of the surface of the uncoated microparticles (Fig. 2A and B) to the CHI-THCPSi (Fig. 2C) and CS/HA-THCPSi (Fig. 2D) coated microparticles, it is noticeable that the biopolymers-modified particle surfaces' were smoother than the surface of bare THCPSi microparticles, due to the surface covering by the layer of the biopolymer.

3.2. Drug loading degree and in vitro release studies

Table 1 shows the loading degrees (w-%) of RSV and VCM loaded in coated and uncoated THCPSi microparticles (53–75 and 25–53 μm). No significant differences were found between the drugs loaded into bare THCPSi particles and the drugs loaded into the biopolymer-coated particles.

In order to evaluate the release profiles of RSV and VCM from the loaded THCPSi microparticles, HPLC analysis was performed. Fig. 3 shows the dissolution profiles of the pure drugs (RSV and VCM) at pH 5.5 and 37 °C, as well as the drug release profiles from the loaded bare THCPSi microparticles (RSV/VCM-THCPSi) and the drug-loaded biopolymer-coated microparticles (RSV/VCM-CHI-THCPSi and RSV/VCM-CS/HA-THCPSi). An extended release of RSV (Fig. 3A) was observed for all the prepared PSi particles, comparatively to that observed for the pure drug, an effect that can be explained by the confinement of the drug molecules within the small pores of the porous matrix of the PSi microparticles,

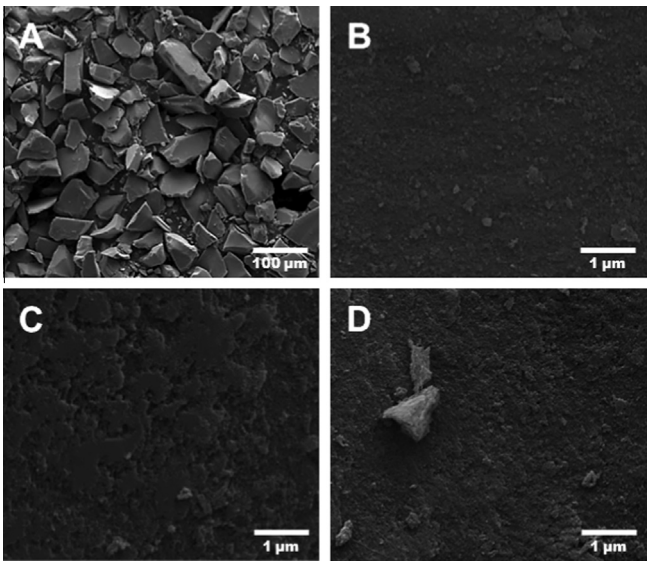

Fig. 2. SEM images of the bare THCPSi (A and B), CHI-THCPSi (C) microparticles and CS/HA-THCPSi (D). Scale bars are 100 µm (A) and 1 µm (B–D). Magnifications are 500× (A) and 50,000× (B–D).

Table 1
Loading degrees (w-%) of VCM and RSV loaded into the uncoated and coated THCPSi microparticles determined by HPLC.

Microparticles	VCM (w-%)	RSV (w-%)
THCPSi	16.50 ± 0.33	2.55 ± 0.05
CHI-THCPSi	15.28 ± 0.31	3.45 ± 0.07
CS/HA-THCPSi	13.12 ± 0.26	3.42 ± 0.07

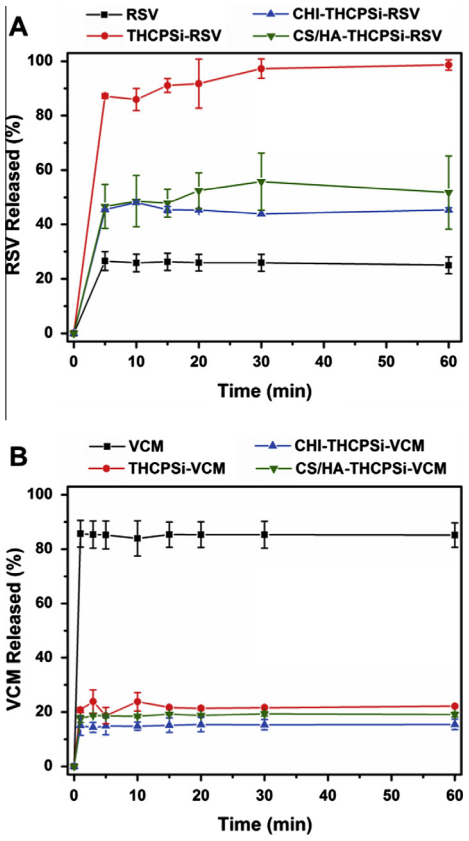

Fig. 3. Release profiles of RSV (A) and VCM (B) from the THCPSi (red), CHI-THCPSi (blue) and CS/HA-THCPSi (green) microparticles. The experiments were performed in MES at pH 5.5 and 32 °C. Error bars represent mean ± s.d. ($n \geqslant 4$). (For interpretation of the references to color in this figure legend, the reader is referred to the web version of this article.)

therefore hindering the nucleation and recrystallization phenomena through physical confinement [26,41,48]. The results showed an initial burst release for the bare THCPSi microparticles, as well as for their CHI and CS/HA-coated counterparts, since the amount of RSV released from the particles reached a *plateau* state within 5 min. Approximately 45.4% and 46.6% of the RSV loaded inside the CHI-THCPSi and CS/HA-THCPSi microparticles, respectively, was released, which can be explained by both the low solubility of the drug in the releasing medium, and a possible interaction between the drug and the polymeric films adsorbed onto the surface of the THCPSi microparticles resulting on the entrapment of the drug molecules within the porous matrix. In the case of VCM-loaded PSi microparticles (Fig. 3B), no difference was observed between uncoated and biopolymer-coated PSi microparticles, which showed a burst release of 22.1% (THCPSi), 15.1% (CHI-THCPSi) and 19.0% (CS/HA-THCPSi) of the VCM loaded within 5 min. Similar release trends for both drugs were observed up to 3 h (results not shown).

3.3. Cell viability/proliferation studies

In order to evaluate the effects of the different biopolymer-modified THCPSi microparticles on the cell viability, a luminescence-based assay was performed on fibroblasts. Fig. 4 shows the results of the cell viability assay on fibroblasts after 24 h (A), 48 h (B), 72 h (C), and 96 h (D) incubated with solutions of CHI and CS/HA mixture at the concentration of 250 µg/mL, bare THCPSi microparticles, as well as different biopolymer-coated THCPSi microparticles (CHI-THCPSi and CS/HA-THCPSi), prepared in four concentrations (25, 100, 500, and 1000 µg/mL) using 10% DMEM medium. DMEM and Triton® X-100 (1%) were used as positive and negative controls, respectively. From the results presented in Fig. 4, both the surface chemical composition and the concentration of the THCPSi microparticles had a significant influence in their cytotoxicity. The effect of the surface chemistry of THCPSi on their biocompatibility, in respect of other PSi-based materials, may be attributed to their hydrophobic nature, which affects the way they interact with the cells [27]. Contrarily, the results showed that none of the biopolymer-modified THCPSi microparticles caused significant cytotoxicity at the particle concentrations and different time points tested, except for the concentrations of 500 and 1000 µg/mL after 24 h incubation. Moreover, compared to the uncoated microparticles, the coated PSi microparticles seem to be less toxic, particularly after 96 h incubation, a feature that can be attributed to the high biocompatibility of the biopolymers adsorbed on the surface of these particles, as elucidated by the high survival of the fibroblasts incubated with the biopolymers solutions in all the time points tested [10,11,20].

3.4. ROS production studies

Next, we evaluated the possible intracellular formation of ROS by the fibroblast cells, when exposed to different modified THCPSi microparticles. For this purpose, a ROS production assay was also performed as shown in Fig. 5. The results of the ROS production assay on fibroblasts after 6 h of incubation with bare (THCPSi) and biopolymer-coated (CHI-THCPSi and CS/HA-THCPSi) microparticles prepared in three concentrations (25, 100, and 500 µg/mL) in HBSS buffer (pH 7.4) and compared to the negative (HBSS buffer) and positive (H_2O_2) controls, showed that none of the modified

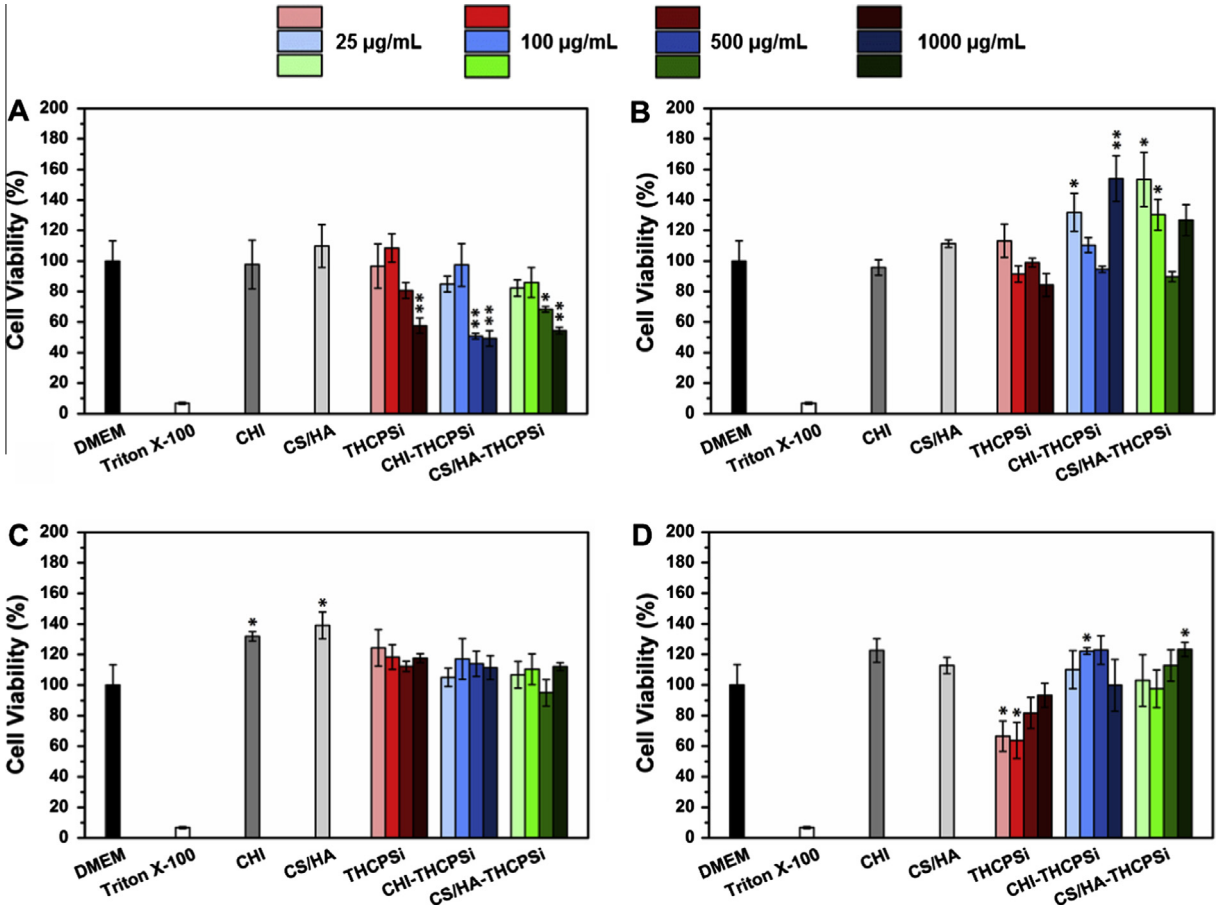

Fig. 4. Fibroblasts viability (%) determined by an ATP-based luminescence assay after 24 h (A), 48 h (B), 72 h (C), and 96 h (D) of incubation at 37 °C with CHI (dark gray) and CS/HA mixture (light gray) solutions, at the concentration of 250 µg/mL, and with different concentrations of THCPSi (red), CHI-coated THCPSi (blue), and CS/HA-THCPSi microparticles (green). Cells cultured with HBSS (pH 7.4) and with 1% Triton X-100 were used as positive and negative controls, respectively. Errors bars represent mean ± s.d. ($n \geqslant 3$). Statistical analysis was performed against the negative control, by means of the Student's *t*-test with the level of significance set at probabilities of $^{*}p < 0.05$ and $^{**}p < 0.01$. (For interpretation of the references to color in this figure legend, the reader is referred to the web version of this article.)

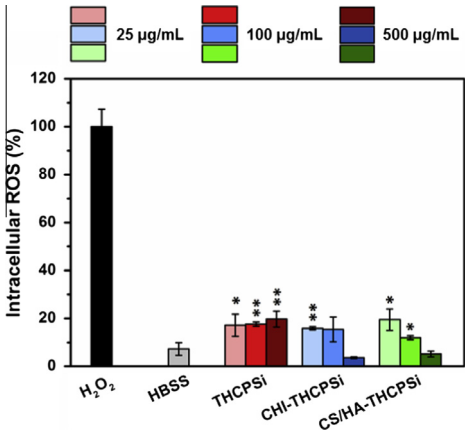

Fig. 5. Fibroblasts intracellular ROS production (%) determined by a fluorescence assay after 6 h incubation with bare (THCPSi) and biopolymer-coated (CHI-THCPSi and CS/HA-THCPSi) microparticles at different concentrations (25, 100, and 500 µg/mL). Cells cultured with hydrogen peroxide (H_2O_2, 0.09%) and with HBSS (pH 7.4) were used as positive and negative controls, respectively. Error bars represent mean ± s.d. ($n \geqslant 3$). Statistical analysis was performed against the negative control, by means of the Student's *t*-test with the level of significance set at probabilities of $^{*}p < 0.05$ and $^{**}p < 0.01$. (For interpretation of the references to color in this figure legend, the reader is referred to the web version of this article.)

THCPSi microparticles induced significant ROS production at the concentrations tested. Therefore, THCPSi microparticles did not induce toxicity via cellular stimulation of ROS production, as in the case of other PSi-based [27] and related materials [49]. Contrarily, a slightly decreased intracellular ROS production was noticed for high concentrations of both CHI-THCPSi and CS/HA-THCPSi microparticles, which can be substantiated on the antioxidant properties of the biopolymers used on the coating of the THCPSi microparticles [50–54]. An increase of ROS species will affect negatively the wound healing process [55], and thus, these results support the potential suitability of the THCPSi microparticles for wound healing applications.

4. Conclusions

During the last years, the complexity of events involved in the wound healing process has required alternative treatments to the conventional ones. In this context, the use of biopolymer-based composites has led to a great incentive for the development of research for wound healing applications. PSi-based materials have several remarkable properties that revealed to be relevant and applicable for drug delivery purposes. Herein, we report the preparation of biopolymer-coated PSi microparticles loaded with two model drugs, VCM and RSV. The viability and proliferation profiles of a fibroblast cell line exposed to the prepared biopolymer-modified PSi microparticles revealed to be less toxic at different concentrations and time points tested compared to the uncoated microparticles. Moreover, the ROS levels produced by the

fibroblasts, when exposed to the bare and biopolymer-coated PSi microparticles, showed that the modified PSi microparticles did not induce significant ROS production at the concentrations tested on the fibroblast cells, and inclusively presented a slight antioxidant effect when incubated with the fibroblasts at high concentrations. Moreover, the coating of the PSi microparticles with biopolymers successfully resulted in an extended release of both VCM and RSV drugs. Although this study demonstrates the high potential of the developed microparticles as drug delivery microsystems for future applications in wound healing, there is still the need for additional testing of their efficacy in a physiopathological scenario. Overall, the biopolymer-based PSi microparticles herein developed represent a suitable and promising platform for wound healing applications.

Conflict of interest

The authors declare no competing financial interest.

Acknowledgements

Dr. Hélder A. Santos acknowledges financial support from the Academy of Finland (Decision No. 252215), the University of Helsinki Research Funds and the Biocentrum Helsinki. Dr. Carmen Escobedo-Lucea (Division of Pharmaceutical Biosciences, Faculty of Pharmacy, University of Helsinki, Finland) is acknowledged for generously providing the fibroblast cells.

References

[1] G. Crovetti, G. Martinelli, M. Issi, M. Barone, M. Guizzardi, B. Campanati, M. Moroni, A. Carabelli, Platelet gel for healing cutaneous chronic wounds, Transfus. Apher. Sci. 30 (2) (2004) 145–151.
[2] J.S. Boateng, K.H. Matthews, H.N.E. Stevens, G.M. Eccleston, Wound healing dressings and drug delivery systems: a review, J. Pharm. Sci. 97 (8) (2008) 2892–2923.
[3] J.M. Rhett, G.S. Ghatnekar, J.A. Palatinus, M. O'Quinn, M.J. Yost, R.G. Gourdie, Novel therapies for scar reduction and regenerative healing of skin wounds, Trends Biotechnol. 26 (4) (2008) 173–180.
[4] R. Muzzarelli, Chitins and chitosans for the repair of wounded skin, nerve, cartilage and bone, Carbohydr. Polym. 76 (2) (2009) 167–182.
[5] J.D. Esko, K. Kimata, U. Lindahl, Proteoglycans and sulfated glycosaminoglycans, in: A. Varki, R.D. Cummings, J.D. Esko, H.H. Freeze, P. Stanley, C.R. Bertozzi, G.W. Hart, M.E. Etzler (Eds.), Essentials of Glycobiology, second ed., Cold Spring Harbor, NY, 2009.
[6] W.Y. Chen, G. Abatangelo, Functions of hyaluronan in wound repair, Wound Repair Regen. 7 (2) (1999) 79–89.
[7] G. Weindl, M. Schaller, M. Schafer-Korting, H.C. Korting, Hyaluronic acid in the treatment and prevention of skin diseases: molecular biological, pharmaceutical and clinical aspects, Skin Pharmacol. Physiol. 17 (5) (2004) 207–213.
[8] F.L. Mi, Y.B. Wu, S.S. Shyu, J.Y. Schoung, Y.B. Huang, Y.H. Tsai, J.Y. Hao, Control of wound infections using a bilayer chitosan wound dressing with sustainable antibiotic delivery, J. Biomed. Mater. Res. 59 (3) (2002) 438–449.
[9] K. Mizuno, K. Yamamura, K. Yano, T. Osada, S. Saeki, N. Takimoto, T. Sakurai, Y. Nimura, Effect of chitosan film containing basic fibroblast growth factor on wound healing in genetically diabetic mice, J. Biomed. Mater. Res. A 64A (1) (2003) 177–181.
[10] M.N.V.R. Kumar, A review of chitin and chitosan applications, React. Funct. Polym. 46 (1) (2000) 1–27.
[11] T.H. Dai, M. Tanaka, Y.Y. Huang, M.R. Hamblin, Chitosan preparations for wounds and burns: antimicrobial and wound-healing effects, Expert Rev. Anti Infect. Ther. 9 (7) (2011) 857–879.
[12] C. Alemdaroglu, Z. Degim, N. Celebi, F. Zor, S. Ozturk, D. Erdogan, An investigation on burn wound healing in rats with chitosan gel formulation containing epidermal growth factor, Burns 32 (3) (2006) 319–327.
[13] H.A. Santos, M.S. Pires, J.A. Vilela, T.M. Santos, J.L. Faccini, C.D. Baldani, S.M. Thome, A. Sanavria, C.L. Massard, Detection of *Anaplasma phagocytophilum* in Brazilian dogs by real-time polymerase chain reaction, J. Vet. Diagn. Invest. 23 (4) (2011) 770–774.
[14] X.H. Zou, W.C. Foong, T. Cao, B.H. Bay, H.W. Ouyang, G.W. Yip, Chondroitin sulfate in palatal wound healing, J. Dent. Res. 83 (11) (2004) 880–885.
[15] A.E.I. Proudfoot, The biological relevance of chemokine–proteoglycan interactions, Biochem. Soc. Trans. 34 (Pt 3) (2006) 422–426.
[16] A.N. Alexopoulou, H.A.B. Multhaupt, J.R. Couchman, Syndecans in wound healing, inflammation and vascular biology, Int. J. Biochem. Cell Biol. 39 (3) (2007) 505–528.
[17] K.J. Wang, N.H. Dan, S.W. Xiao, Y.C. Ye, W.H. Dan, Preparation and characterization of collagen–chitosan–chondroitin sulfate composite membranes, J. Membr. Biol. 245 (11) (2012) 707–716.
[18] M. Akmal, A. Singh, A. Anand, A. Kesani, N. Aslam, A. Goodship, G. Bentley, The effects of hyaluronic acid on articular chondrocytes, J. Bone Joint Surg. Br. 87B (8) (2005) 1143–1149.
[19] K.N. Antonas, K.D. Muirden, J.R.E. Fraser, Distribution of biologically labeled radioactive hyaluronic-acid injected into joints, Ann. Rheum. Dis. 32 (2) (1973) 103–111.
[20] J. Necas, L. Bartosikova, P. Brauner, J. Kolar, Hyaluronic acid (hyaluronan): a review, Vet. Med. – Czech 53 (8) (2008) 397–411.
[21] V. Voinchet, P. Vasseur, J. Kern, Efficacy and safety of hyaluronic acid in the management of acute wounds, Am. J. Clin. Dermatol. 7 (6) (2006) 353–357.
[22] H.A. Santos, L. Peltonen, T. Limnell, J. Hirvonen, Mesoporous materials and nanocrystals for enhancing the dissolution behavior of poorly water-soluble drugs, Curr. Pharm. Biotechnol. 14 (10) (2014) 926–938.
[23] H.A. Santos, E. Mäkilä, A.J. Airaksinen, L.M. Bimbo, J. Hirvonen, Porous silicon nanoparticles for nanomedicine: preparation and biomedical applications, Nanomedicine 9 (4) (2014) 535–554.
[24] H.A. Santos, L.M. Bimbo, V.P. Lehto, A.J. Airaksinen, J. Salonen, J. Hirvonen, Multifunctional porous silicon for therapeutic drug delivery and imaging, Curr. Drug Discov. Technol. 8 (3) (2011) 228–249.
[25] H.A. Santos, J. Salonen, L.M. Bimbo, V.P. Lehto, L. Peltonen, J. Hirvonen, Mesoporous materials as controlled drug delivery formulations, J. Drug Deliv. Sci. Technol. 21 (2) (2011) 139–155.
[26] J. Salonen, A.M. Kaukonen, J. Hirvonen, V.P. Lehto, Mesoporous silicon in drug delivery applications, J. Pharm. Sci. 97 (2) (2008) 632–653.
[27] H.A. Santos, J. Riikonen, J. Salonen, E. Mäkilä, T. Heikkilä, T. Laaksonen, L. Peltonen, V.P. Lehto, J. Hirvonen, In vitro cytotoxicity of porous silicon microparticles: effect of the particle concentration, surface chemistry and size, Acta Biomater. 6 (7) (2010) 2721–2731.
[28] L.M. Bimbo, M. Sarparanta, H.A. Santos, A.J. Airaksinen, E. Mäkilä, T. Laaksonen, L. Peltonen, V.P. Lehto, J. Hirvonen, J. Salonen, Biocompatibility of thermally hydrocarbonized porous silicon nanoparticles and their biodistribution in rats, ACS Nano 4 (6) (2010) 3023–3032.
[29] L.M. Bimbo, E. Mäkilä, T. Laaksonen, V.P. Lehto, J. Salonen, J. Hirvonen, H.A. Santos, Drug permeation across intestinal epithelial cells using porous silicon nanoparticles, Biomaterials 32 (10) (2011) 2625–2633.
[30] S.P. Low, N.H. Voelcker, L.T. Canham, K.A. Williams, The biocompatibility of porous silicon in tissues of the eye, Biomaterials 30 (15) (2009) 2873–2880.
[31] T. Tanaka, B. Godin, R. Bhavane, R. Nieves-Alicea, J. Gu, X. Liu, C. Chiappini, J.R. Fakhoury, S. Amra, A. Ewing, Q. Li, I.J. Fidler, M. Ferrari, In vivo evaluation of safety of nanoporous silicon carriers following single and multiple dose intravenous administrations in mice, Int. J. Pharm. 402 (1–2) (2010) 190–197.
[32] H.W. Jaffe, J.S. Lewis, P.J. Wiesner, Vancomycin-sensitive *Neisseria gonorrheae*, J. Infect. Dis. 144 (2) (1981) 198–200.
[33] C.K. Sen, S. Khanna, G. Gordillo, D. Bagchi, M. Bagchi, S. Roy, Oxygen, oxidants, and antioxidants in wound healing: an emerging paradigm, Ann. N. Y. Acad. Sci. 957 (2002) 239–249.
[34] I. Yaman, H. Derici, C. Kara, E. Kamer, G. Diniz, R. Ortac, O. Sayin, Effects of resveratrol on incisional wound healing in rats, Surg. Today 43 (12) (2013) 1433–1438.
[35] E. Pastor, E. Matveeva, A. Valle-Gallego, F.M. Goycoolea, M. Garcia-Fuentes, Protein delivery based on uncoated and chitosan-coated mesoporous silicon microparticles, Colloids Surf. B: Biointerfaces 88 (2) (2011) 601–609.
[36] J.Q. Xi, J. Qin, L. Fan, Chondroitin sulfate functionalized mesostructured silica nanoparticles as biocompatible carriers for drug delivery, Int. J. Nanomed. 7 (2012) 5235–5247.
[37] M.H. Yu, S. Jambhrunkar, P. Thorn, J.Z. Chen, W.Y. Gu, C.Z. Yu, Hyaluronic acid modified mesoporous silica nanoparticles for targeted drug delivery to CD44-overexpressing cancer cells, Nanoscale 5 (1) (2013) 178–183.
[38] M. Kovalainen, J. Mönkäre, M. Kaasalainen, J. Riikonen, V.P. Lehto, J. Salonen, K.H. Herzig, K. Järvinen, Development of porous silicon nanocarriers for parenteral peptide delivery, Mol. Pharmaceutics 10 (1) (2013) 353–359.
[39] J. Salonen, M. Björkqvist, E. Laine, L. Niinistö, Stabilization of porous silicon surface by thermal decomposition of acetylene, Appl. Surf. Sci. 225 (1–4) (2004) 389–394.
[40] S. Brunauer, P.H. Emmett, E. Teller, Adsorption of gases in multimolecular layers, J. Am. Chem. Soc. 60 (2) (1938) 309–319.
[41] E. Mäkilä, M.P. Ferreira, H. Kivela, S.M. Niemi, A. Correia, M.A. Shahbazi, J. Kauppila, J. Hirvonen, H.A. Santos, J. Salonen, Confinement effects on drugs in thermally hydrocarbonized porous silicon, Langmuir: ACS J. Surf. Colloids 30 (8) (2014) 2196–2205.
[42] S. Schreml, R.M. Szeimies, S. Karrer, J. Heinlin, M. Landthaler, P. Babilas, The impact of the pH value on skin integrity and cutaneous wound healing, J. Eur. Acad. Dermatol. Venereol. 24 (4) (2010) 373–378.
[43] N. Shrestha, M.A. Shahbazi, F. Araujo, H. Zhang, E.M. Mäkilä, J. Kauppila, B. Sarmento, J.J. Salonen, J.T. Hirvonen, H.A. Santos, Chitosan-modified porous silicon microparticles for enhanced permeability of insulin across intestinal cell monolayers, Biomaterials 35 (25) (2014) 7172–7179.
[44] Y. Hattori, H. Yamasaku, Y. Maitani, Anionic polymer-coated lipoplex for safe gene delivery into tumor by systemic injection, J. Drug Target. 21 (7) (2013) 639–647.
[45] X. Fei Liu, Y. Lin Guan, D. Zhi Yang, Z. Li, K. De Yao, Antibacterial action of chitosan and carboxymethylated chitosan, J. Appl. Polym. Sci. 79 (7) (2001) 1324–1335.

[46] K. Potter, L.H. Kidder, I.W. Levin, E.N. Lewis, R.G.S. Spencer, Imaging of collagen and proteoglycan in cartilage sections using Fourier transform infrared spectral imaging, Arthritis Rheum. 44 (4) (2001) 846–855.
[47] M. Mason, K.P. Vercruysse, K.R. Kirker, R. Frisch, D.M. Marecak, C.D. Prestwich, W.G. Pitt, Attachment of hyaluronic acid to polypropylene, polystyrene, and polytetrafluoroethylene, Biomaterials 21 (1) (2000) 31–36.
[48] J. Salonen, L. Laitinen, A.M. Kaukonen, J. Tuura, M. Björkqvist, T. Heikkilä, K. Vaha-Heikkilä, J. Hirvonen, V.P. Lehto, Mesoporous silicon microparticles for oral drug delivery: loading and release of five model drugs, J. Controlled Release 108 (2–3) (2005) 362–374.
[49] B. Fubini, A. Hubbard, Reactive oxygen species (ROS) and reactive nitrogen species (RNS) generation by silica in inflammation and fibrosis, Free Radic. Biol. Med. 34 (12) (2003) 1507–1516.
[50] J. Egea, A.G. Garcia, J. Verges, E. Montell, M.G. Lopez, Antioxidant, antiinflammatory and neuroprotective actions of chondroitin sulfate and proteoglycans, Osteoarthritis and cartilage/OARS, Osteoarthritis Res. Soc. 18 (Suppl. 1) (2010) S24–S27.
[51] G.M. Campo, A. Avenoso, A. D'Ascola, S. Campo, A.M. Ferlazzo, D. Sama, A. Calatroni, Purified human plasma glycosaminoglycans limit oxidative injury induced by iron plus ascorbate in skin fibroblast cultures, Toxicol. In Vitro 19 (5) (2005) 561–572.
[52] C.H. Xue, G.L. Yu, T. Hirata, J. Terao, H. Lin, Antioxidative activities of several marine polysaccharides evaluated in a phosphatidylcholine-liposomal suspension and organic solvents, Biosci. Biotechnol. Biochem. 62 (2) (1998) 206–209.
[53] M.T. Chiang, H.T. Yao, H.C. Chen, Effect of dietary chitosans with different viscosity on plasma lipids and lipid peroxidation in rats fed on a diet enriched with cholesterol, Biosci. Biotechnol. Biochem. 64 (5) (2000) 965–971.
[54] M. Anraku, M. Tanaka, A. Hiraga, K. Nagumo, T. Imafuku, Y. Maezaki, D. Iohara, K. Uekama, H. Watanabe, F. Hirayama, T. Maruyama, M. Otagiri, Effects of chitosan on oxidative stress and related factors in hemodialysis patients, Carbohydr. Polym. 112 (2014) 152–157.
[55] P.G. Rodriguez, F.N. Felix, D.T. Woodley, E.K. Shim, The role of oxygen in wound healing: a review of the literature, Dermatol. Surg. 34 (9) (2008) 1159–1169.